

Crack Bridging. Lecture 2

Lecture 1 (<http://imechanica.org/node/7948>) introduced the crack bridging model. The model is also known as the cohesive-zone model, the Barenblatt model, or the Dugdale model. The model consists of two main ingredients:

- The process of separation of the body is modeled by a traction-separation curve;
- The process of deformation in the body is modeled by a field theory, such as the linear elastic theory.

For a body of a given configuration and traction-separation curve, the model results in a boundary-value problem. A large number of such boundary-value problems have been solved. These problems can also be solved by commercial finite element software, such as ABAQUS. The limited time in this course will only allow us to describe a few examples.

Lecture 1 focused on small-scale bridging, when the body contains a pre-existing crack, and the size of the bridging zone is much smaller than the characteristic length of the body (e.g., the length of the crack and of the ligament). Under the small-scale bridging condition, the external boundary conditions of the body can be represented by a single parameter, the energy release rate. Consequently, the Griffith (1921) approach—as extended by Irwin, Orowan, Rivlin and Thomas in 1950s—can be used to determine the fracture energy. Once determined, the fracture energy of a material can be used to predict the failure of bodies of the same material but different configurations.

This lecture is devoted to large-scale bridging. When the size of the bridging zone is comparable to, or even larger than, the characteristic length of a body, the external boundary conditions cannot be represented by the energy release rate alone. The Griffith approach fails.

The crack-bridging model, however, applies under the large-scale bridging conditions. Within the crack-bridging model, the traction-separation curve characterizes the resistance of a material to fracture. The traction-separation curve can be determined by a combination of computation and experimental measurement. Once determined, the traction-separation curve of a material can be used to predict failure of specimens of the same material but different configurations.

Ceramic-matrix composite. Consider, for example, a composite of ceramic fibers embedded in a ceramic matrix. When the composite is subject to a load along the direction of the fibers, a crack may propagate in the matrix, leaving the fibers intact. The composite resists the extension of the crack by two processes:

1. The fibers slide relative to the matrix, and bridge the crack.
2. The atomic bonds of the matrix break at the front of the crack.

The bridging fibers are represented a traction-separation curve $\sigma(\delta)$, as described at the end of Lecture 1. The atomic bond breaking process at the front of the crack is represented by fracture energy Γ_{tip} , which is roughly the fracture energy of the matrix.

Crack-bridging model as a boundary-value problem. Let us list parameters that specify the crack bridging model. The model consists of two main ingredients:

- The process of separation of the body is modeled by an array of springs, characterized by a traction-separation curve, $\sigma(\delta)$;
- The process of deformation in the body is modeled by the linear elastic theory, characterized by Young's modulus E and Poisson's ratio ν .

The springs and the body together constitute a boundary-value problem. The boundary conditions are characterized by

- Lengths such as the overall size of the body, w ;
- The size of a stress concentrator, such as the radius of a hole or the length of a pre-existing crack, a ;
- Applied load, σ_{appl} .

To formulate a boundary-value problem, two other parameters need be prescribed:

- The length of the bridging zone, L .
- The fracture energy at the tip of the bridging zone, Γ_{tip}

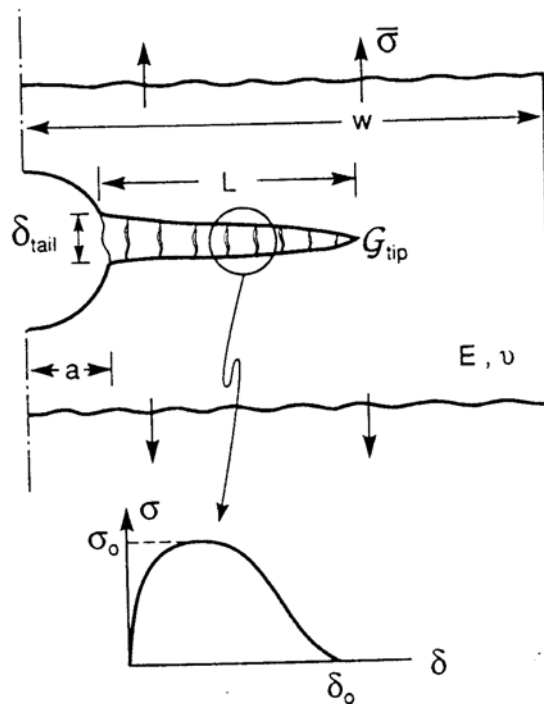


Fig. 1 An inelastic band is viewed as either a bridged crack or an array of continuously distributed dislocations

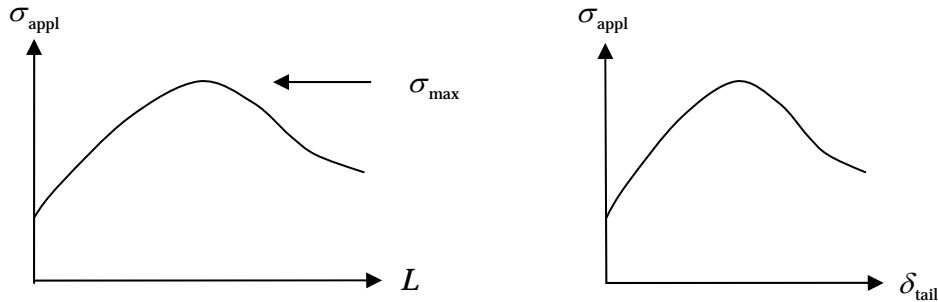
Once a boundary-value problem is solved, what do you want from the solution? Because the springs are nonlinear, the crack-bridging model usually leads to a nonlinear boundary-value problem. For a given σ_{appl} and L , one can solve the boundary-value problem. In particular, one can calculate the following quantities. At the tip of the bridging zone, the energy release rate is

$$G_{\text{tip}} = G(\sigma_{\text{appl}}, L).$$

At the tail of the bridging zone, the separation is

$$\delta_{\text{tail}} = F(\sigma_{\text{appl}}, L).$$

Setting $G_{\text{tip}} = \Gamma_{\text{tip}}$, one can invert the first equation to obtain a function $\sigma_{\text{appl}}(L)$. This function, together with the second equation above, leads to a



function $\sigma_{\text{appl}}(\delta_{\text{tail}})$. Perhaps you are interested in the maximum stress σ_{max} that can be applied to the body.

Scaling. The traction-separation curve sets a scale of traction σ_0 and a scale of separation δ_0 . Under the condition of small-scale bridging, the fracture energy due to bridging is

$$\Gamma_B = \int_0^{\infty} \sigma(\delta) d\delta,$$

and the length of the steady-state bridging zone scales as

$$E\Gamma_B / \sigma_0^2.$$

This length involves material parameters, and is therefore a material parameter itself. We can compare this material length to the length of the pre-existing crack, a . Examine the dimensionless ratio of the two lengths:

$$\frac{a}{E\Gamma_B / \sigma_0^2}.$$

The small-scale bridging condition prevails when

$$\frac{a}{E\Gamma_B / \sigma_0^2} \gg 1.$$

Lecture 1 focuses on the small-scale condition.

This lecture explores the large-scale condition. Under the large-scale bridging condition, the solution to the crack-bridging model may be written in a dimensionless form:

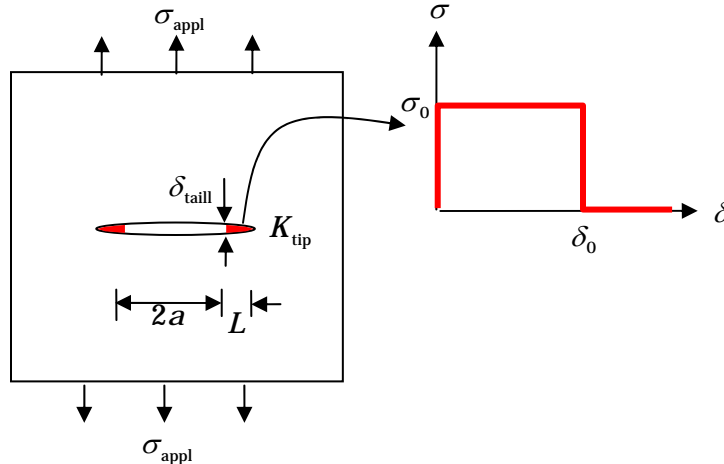
$$\frac{\delta_{\text{tail}}}{a} = f\left(\frac{\sigma_{\text{appl}}}{\sigma_0}, \frac{L}{a}, \frac{a}{E\Gamma_B / \sigma_0^2}\right),$$

$$\frac{G_{\text{tip}}}{\Gamma_B} = g\left(\frac{\sigma_{\text{appl}}}{\sigma_0}, \frac{L}{a}, \frac{a}{E\Gamma_B / \sigma_0^2}\right).$$

Other dimensionless forms are possible.

Dugdale model (1960). An early example of large-scale bridging was introduced by Dugdale (1960). Cut a crack of length $2a$ into a large panel of steel.

Load the panel with a tensile stress, σ_{appl} . As the applied stress increases, yielding zones develop from the edges of the cut. Let L be the length of each yielding zone. Dugdale assumed that the material in the yielding zones had a constant stress σ_0 , approximately the yield strength of the steel. He further assumed that the yielding zones were confined on the plane of the crack, and the material off the plane remained elastic. In effect, he introduced the crack-crack bridging model.



Imagine a crack of total length $2(a+L)$. The solution is a linear superposition of the applied stress, σ_{appl} , and the bridging traction, σ_0 . The stress intensity factor at the “crack tip” is

$$K_{\text{tip}} = \sigma_{\text{appl}} \sqrt{\pi(a+L)} - \sigma_0 \sqrt{\pi(a+L)} \frac{2}{\pi} \cos^{-1} \left(\frac{a}{a+L} \right).$$

Dugdale argued that the stress should be bounded at the “crack tip”, and set

$$K_{\text{tip}} = 0.$$

The above equation leads to

$$\frac{\sigma_{\text{appl}}}{\sigma_0} = \frac{2}{\pi} \cos^{-1} \left(\frac{a}{a+L} \right).$$

Plot $L/(a+L)$ as a function of $\sigma_{\text{appl}}/\sigma_0$ in the interval (0,1). When $\sigma_{\text{appl}}/\sigma_0 = 0$, the yielding zone vanishes. When $\sigma_{\text{appl}}/\sigma_0 = 1$, the yielding zone approaches infinity, so that $L/(a+L) = 1$. Dugdale measured the yielding zone length L as a function of the applied stress σ_{appl} . His experimental data agreed with the calculated curve.

In his original model, Dugdale assumed that as σ_{appl} increased, the yielding zone extended at the front, but did not rupture at the tail. In reality, of course, necking develops along the yielding zone. The tail ruptures when the separation δ_{tail} reaches a limiting value, δ_0 . For a thin panel, the limiting separation is comparable to the thickness of the panel.

Separation at the tail of the bridging zone. The Dugdale model has been extended to analyze rupture (Bilby, Cottrell and Swinden, 1963). The separation at the tail δ_{tail} is also linear in σ_{appl} and σ_0 :

$$\delta_{\text{tail}} = \frac{4\sigma_{\text{appl}}}{E} \sqrt{(a+L)^2 - a^2} - \frac{8\sigma_0}{\pi E} \left[\cos^{-1}\left(\frac{a}{a+L}\right) \sqrt{(a+L)^2 - a^2} - a \log\left(\frac{a+L}{a}\right) \right].$$

The contribution due to σ_{appl} is well known, but that due to σ_0 requires some work to obtain.

Eliminate σ_{appl} from the above, we express δ_{tail} in terms of L :

$$\frac{\delta_{\text{tail}} E}{\sigma_0 a} = \frac{8}{\pi} \log\left(\frac{a+L}{a}\right).$$

The separation at the tail increases with the length of the yielding zone.

Load-carrying capacity of a panel with a pre-existing crack. The above expressions relate δ_{tail} and σ_{appl} , using the length of the bridging zone L as an intermediate variable. When $\delta_{\text{tail}} = \delta_0$, the applied stress reaches the maximum stress σ_{max} that can be sustained by the specimen. This relation reproduces the two limiting cases.

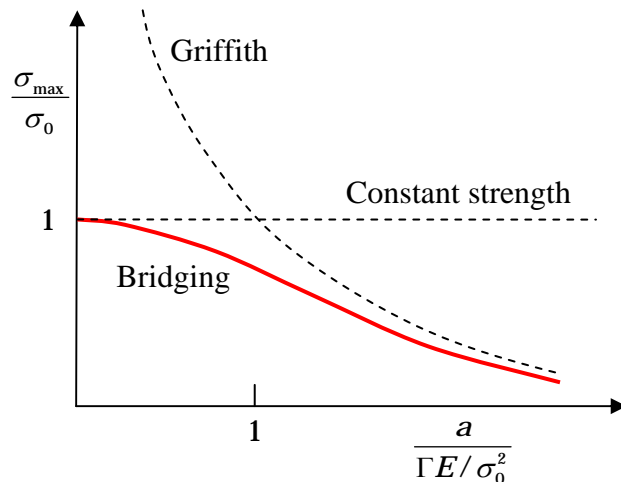
Plot $\sigma_{\text{max}}/\sigma_0$ as a function of $a/(\Gamma E/\sigma_0^2)$. The two asymptotic behaviors are known. When $\frac{a}{\Gamma E/\sigma_0^2} \ll 1$, the strength of the specimen is insensitive to the size of the pre-existing crack, and is given by the strength of the bridges:

$$\sigma_{\text{max}} = \sigma_0.$$

When $\frac{a}{\Gamma E/\sigma_0^2} \gg 1$, the small-scale bridging condition prevails, and the strength of the specimen is sensitive to the size of the pre-existing crack, and is given by the Griffith formula:

$$\sigma_{\text{max}} = \sqrt{\frac{E\Gamma}{\pi a}}.$$

The crack-bridging model bridges the two limits.



Shape of the traction-separation curve. In practice, the shape of the traction-separation curve may not be determined accurately. It is interesting to see how the shape of the traction-separation curve affects the quantities of interest. As an example, Suo, Ho and Gong (1993) showed that the strength of a

specimen containing a pre-existing crack is insensitive to the shape of the traction-separation curve.

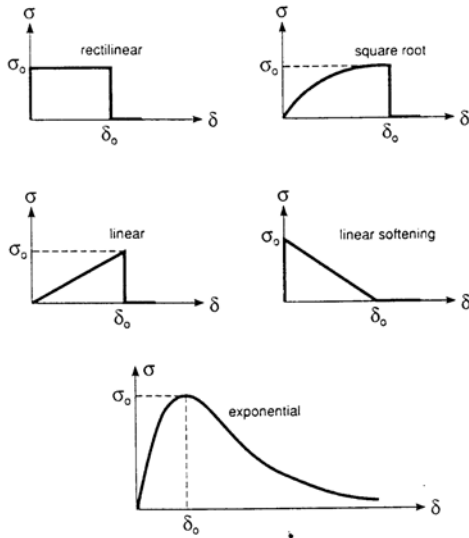


Fig. 2 Idealized bridging laws

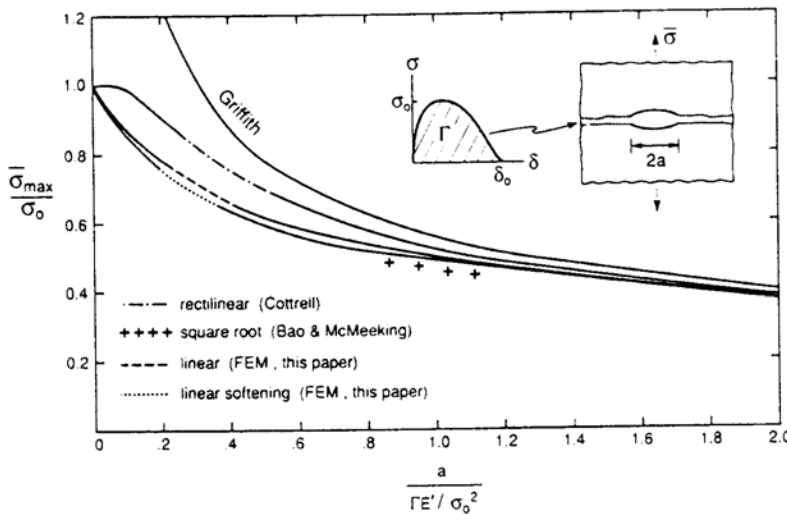


Fig. 7 Notch ductile-to-brittle transition (sharp notch)

Notch sensitivity. Now consider stress concentrators other than a sharp crack. For example, consider a panel with a circular hole whose diameter is small compared to the panel width (Suo, Ho and Gong, 1993). How much load can the panel carry?

The answer depends on materials. For a glass panel, the hole concentrates stress, and reduces the load carrying capacity by a factor 3. Glass is *notch-sensitive*. For a steel panel, plastic deformation removes stress concentration, so that the hole does not affect the load-carrying capacity. Steel is *notch-insensitive*.

The above answer appeals to our intuition, but cannot be totally correct. The answer must vary with the size of the hole. For the glass, if the size of the hole is of atomistic dimension, surely we do not believe it will knock down the load-carrying capacity by a factor 3. For the steel, if the size of the hole is much

larger than the thickness of the panel, the plastic deformation is limited by necking, and the load-carrying capacity will be knocked down.

To analyze these ideas, we model the inelastic deformation by a traction-separation curve. Let the radius of the hole be a . Consider two limits:

- When $\frac{a}{\Gamma E / \sigma_0^2} \ll 1$, $\sigma_{\max} = \sigma_0$ (notch-ductile or notch-insensitive)
- When $\frac{a}{\Gamma E / \sigma_0^2} \gg 1$, $\sigma_{\max} = \sigma_0 / 3$ (notch-brittle or notch-sensitive)

Numerical calculation fills the detail between the two limits. Let the length of the bridging zone be L . For the rectilinear bridging law, linearity requires that

$$\delta_{\text{tail}} E / a = f_1 \sigma_{\text{appl}} - f_2 \sigma_0$$

$$K_{\text{tip}} / \sqrt{a} = f_3 \sigma_{\text{appl}} - f_4 \sigma_0$$

The coefficients f_i depend on L/a , and are determined by solving the boundary-value problem using the finite element method. Require that the stress be bounded, so that $K_{\text{tip}} = 0$, and

$$\sigma_{\text{appl}} / \sigma_0 = f_4 / f_3,$$

The separation at the tail of the bridging zone is

$$\delta_{\text{tail}} E / \sigma_0 a = f_1 f_4 / f_3 - f_2.$$

Consequently, one can plot σ_{appl} versus δ_{tail} . The maximum stress σ_{\max} within the interval $0 < \delta_{\text{tail}} \leq \delta_0$ determines the load-carrying capacity.

The above procedure is good for any other stress concentrators, such as a sharp notch, a corner, etc.

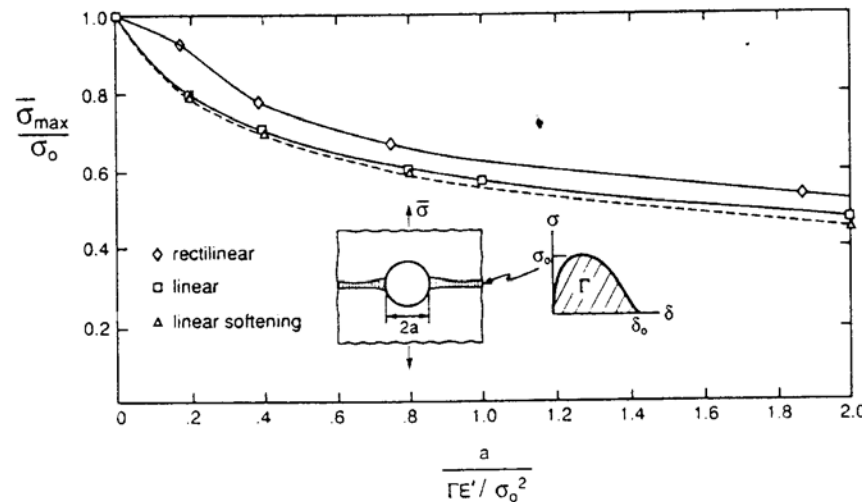


Fig. 8 Notch ductile-to-brittle transition (circular hole)

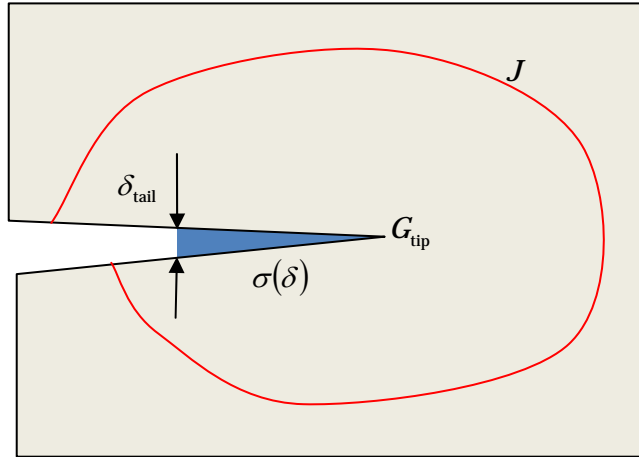
Use the traction-separation curve to predict fracture. Both Γ_{tip} and $\sigma(\delta)$ are material properties, assumed to be independent of the configuration of the specimen. That is, we can determine Γ_{tip} and $\sigma(\delta)$ by fracturing a specimen of one configuration, and then use the measured Γ_{tip} and

$\sigma(\delta)$ to predict fracture of a specimen of another configuration. You will study an example of this approach in a homework problem based on Thouless et al. (1998). Another excellent example is given by Mohammed and Liechti (2000).

The J integral. The J integral over a contour enclosing the bridging zone is

$$J = G_{\text{tip}} + \int_0^{\delta_{\text{tail}}} \sigma(\delta) d\delta.$$

The value of the J is path-independent, so long as the contour encloses the entire bridging zone.



When the bridging zone moves in the body, new bridges are created at the tip, $G_{\text{tip}} = \Gamma_{\text{tip}}$, and old bridges are broken in the tail, $\delta_{\text{tail}} = \delta_0$, so that the J integral takes the form

$$J = \Gamma_{\text{tip}} + \int_0^{\delta_0} \sigma(\delta) d\delta.$$

This result is valid under both the small-scale and the large-scale bridging conditions.

Under the small-scale bridging condition, the size of the bridging zone is much smaller than the characteristic length of the body. Consequently, an annulus exists, in which the stress field is dominated by the square-root singular field, of the form

$$\sigma_{ij} = E \sqrt{\frac{G}{Er}} f_{ij}(\theta).$$

When the J integral is calculated over a contour falling inside the G -annulus,

$$J = G.$$

Because the J integral is path-independent, the crack bridging model predicts the fracture energy as

$$\Gamma_{ss} = \Gamma_{\text{tip}} + \int_0^{\delta_0} \sigma(\delta) d\delta.$$

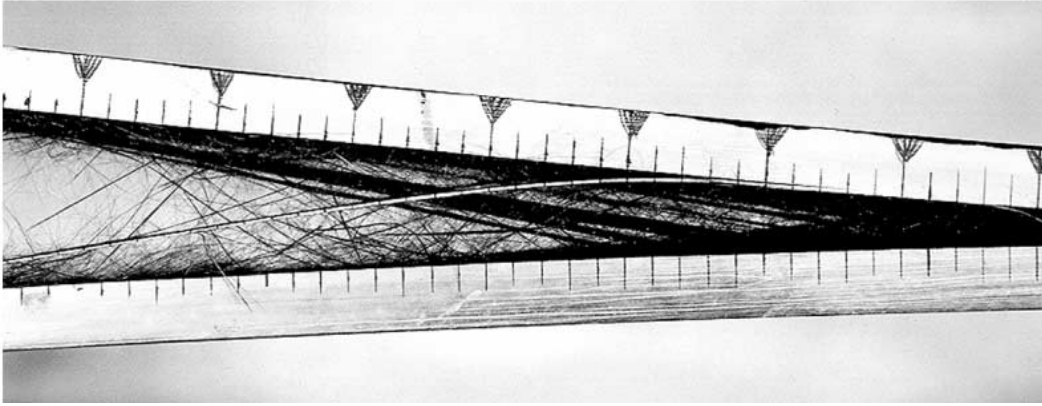
Under the large-scale bridging conditions, the J integral over any path enclosing the bridging zone is still given by

$$J = G_{\text{tip}} + \int_0^{\delta_{\text{tail}}} \sigma(\delta) d\delta.$$

However, because the size of the bridging zone is comparable to, or even larger than, the characteristic size of the specimen, the G -annulus does not exist. We

can no longer use G to represent the external boundary conditions. Nor can we interpret the J integral as the energy release rate.

Delamination R-curve. Spearing and Evans (1992) observed that, during the delamination of a layer of unidirectional composite, fibers crossed over the plane of the crack. See the photo taken from Tamuzs, Tarasovs and Vilks (2001). These crossing-over fibers give rise to apparent fracture energy on the order of 1 kJ/m², a value far exceeding the fracture energy of the matrix. They also observed that the length of the bridging zone could be larger than the thickness of the beam. Under such a large-scale bridging condition, it is troublesome to invoke the concept of fracture energy or R-curve.



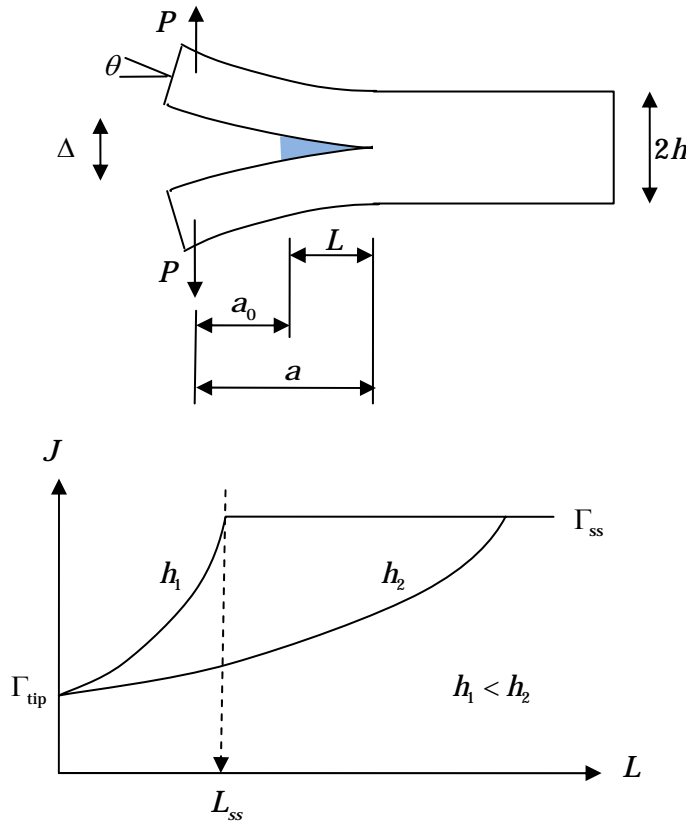
Motivated by this experiment, Suo, Bao and Fan (1992) considered the following idealized situation. The double-cantilever beams are subject to a pair of moment (per unit thickness), M . The thickness of each beam is h . Taking the J integral over the external boundary of the specimen, we obtain that

$$J = \frac{12M^2}{Eh^3}.$$

This J integral should equal that calculated by using the traction-separation curve:

$$J = G_{\text{tip}} + \int_0^{\delta_{\text{tail}}} \sigma(\delta) d\delta.$$

As the applied moment M increases, the J integral also increases. The layer of the composite is cut with a crack of length a_0 . When $J < \Gamma_{\text{tip}}$, the precut crack remains stationary. When $J > \Gamma_{\text{tip}}$, the crack extends, leaving a wake bridged by cross-over fibers. When $J = \Gamma_{\text{ss}}$, the bridging zone translates in the composite, with the front of the zone advancing in the composite, and the tail of zone becomes essentially traction-free. While both Γ_{tip} and Γ_{ss} are independent of the thickness of the layer, the size of the bridging zone needed to attain the steady state, L_{ss} , increases with the thickness of the layer. Consequently, under the large-scale bridging condition, the resistance curve is not a material property, but varies with the thickness of the specimen.



Calculating R-curves. The resistance curves can be calculated once a traction-separation curve is prescribed. It is possible, at least approximately, to determine the traction-separation curve from the R-curve measured from one specimen, and then use the traction-separation curve to predict the R-curve of another specimen.

As an example, consider the double-cantilever beams. Suo, Bao and Fan (1992) considered several idealized traction-separation curves. Here we will discuss the rectilinear traction-separation relation. Linearity and dimensional consideration suggest that

$$\sqrt{\frac{J}{E}} = \sqrt{\frac{\Gamma_{tip}}{E}} + \alpha \frac{\sqrt{3L^2\sigma_0}}{\sqrt{h^3}},$$

where the dimensionless parameter α is a function of a single variable, L/h . The value calculated by using ABAQUS is listed below. The above equation is plotted as a dimensionless R-curve. Note that the R-curves depend on thickness of the beams, and are not material properties.

L/h	0.5	1.0	1.5	2.0	3.0	3.5	4.0	10.0	∞
a	4.89	2.60	2.01	1.74	1.58	1.48	1.35	1.14	1.00

The curves plotted in the figure assumes that

$$\Gamma_{tip} < J < \Gamma_{tip} + \sigma_0\delta_0.$$

When $J < \Gamma_{\text{tip}}$, the bridging zone is absent. When $J = \Gamma_{\text{tip}} + \sigma_0 \delta_0$, this equation gives the steady state fracture resistance, namely, a horizontal line in the figure.

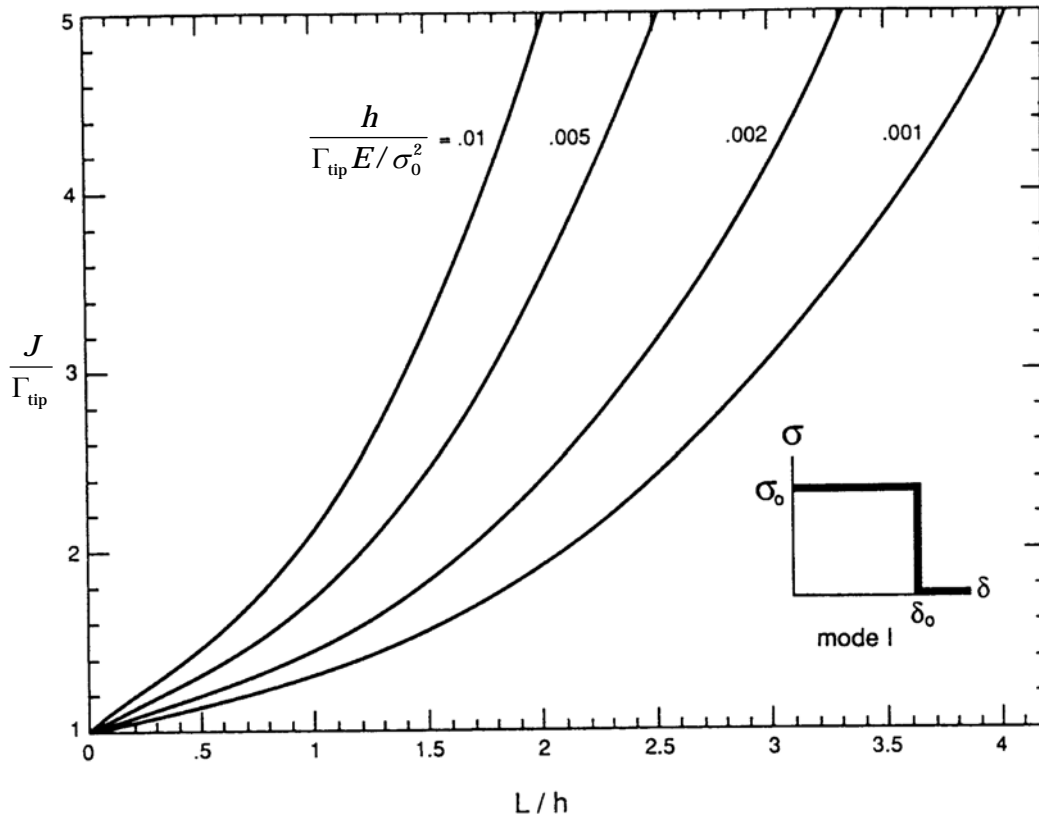


FIG. 7. Dimensionless R -curves predicted using the rigid plastic damage response (mode I).

Use of the J integral in experimental determination of the traction-separation curve. The J integral can be used to aid the experimental determination of the traction-separation curve. Under the large-scale bridging conditions, the J integral is still given by

$$J = G_{\text{tip}} + \int_0^{\delta_{\text{tail}}} \sigma(\delta) d\delta.$$

As the applied load increases, the front of the crack moves, $G_{\text{tip}} = \Gamma_{\text{tip}}$, and the separation δ_{tail} at the tail of the bridging zone increases. Differentiate the above equation with respect to δ_{tail} , we obtain that

$$\sigma(\delta_{\text{tail}}) = \frac{dJ(\delta_{\text{tail}})}{d\delta_{\text{tail}}}.$$

This expression gives the traction-separation curve if experimental determination allow us to determine the J integral as a function of δ_{tail} .

Recall the definition of the J integral (<http://imechanica.org/node/7836>):

$$J = \int (WN_1 - T_i F_n) dL.$$

It would be difficult to determine J through experimental determination of all the field variables involved. However, in specimens of certain configurations, the J

integral relates to quantities that can be determined readily in experiments. Several examples are given below.

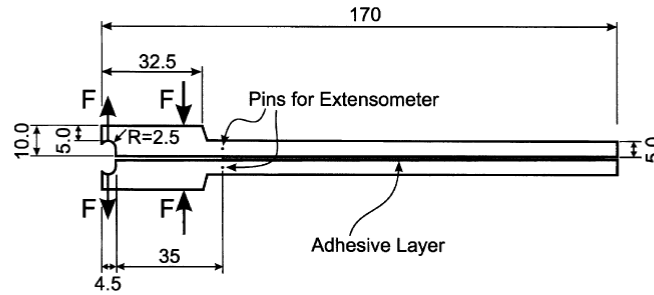
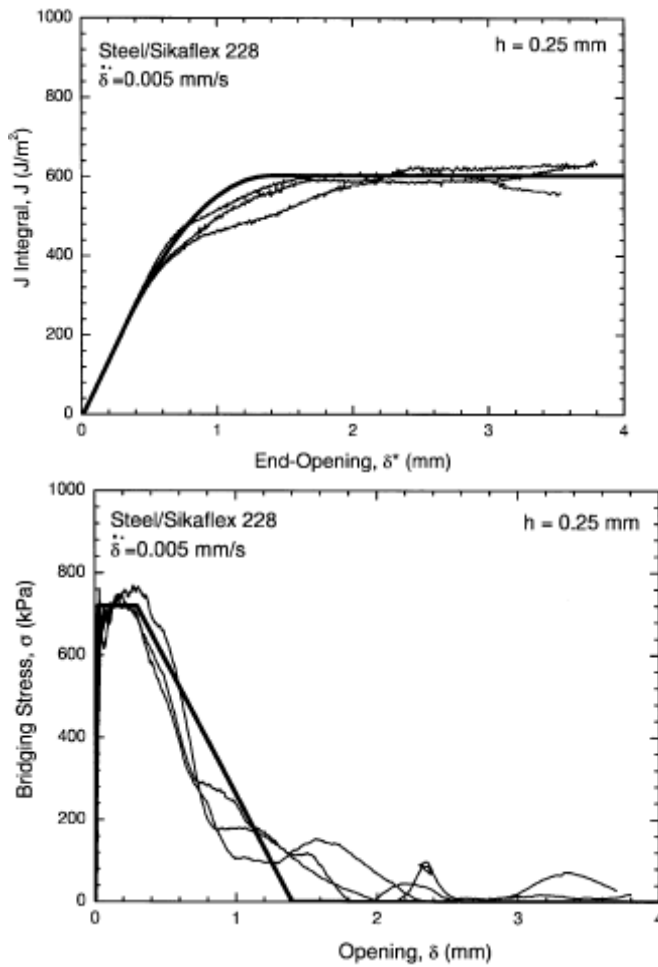


Fig. 3. Schematics showing dimensions (in mm) of the DCB-specimens as well as the applied forces, F , that create the pure bending moments.



Double-cantilever beams subject to pure bending moments. The double-cantilever beams are subject to a pair of bending moments (per unit thickness), M . The thickness of each beam is h . Taking the J integral over the external boundary of the specimen, we obtain that

$$J = \frac{12 M^2}{E h^3}.$$

One can measure δ_{tail} as a function of the applied moment M . This allows one to determine the function $J(\delta_{\text{tail}})$.

This procedure was suggested by Suo, Bao and Fan (1992), and was demonstrated experimentally by Sorensen and Jacobsen (1998). The following figures are taken from Sorensen (2002).

Double-cantilever beams subject to forces. When the double-cantilever beams are subjected to a force P (force per unit width), the J integral over the external boundary is given by (Paris and Paris, 1988):

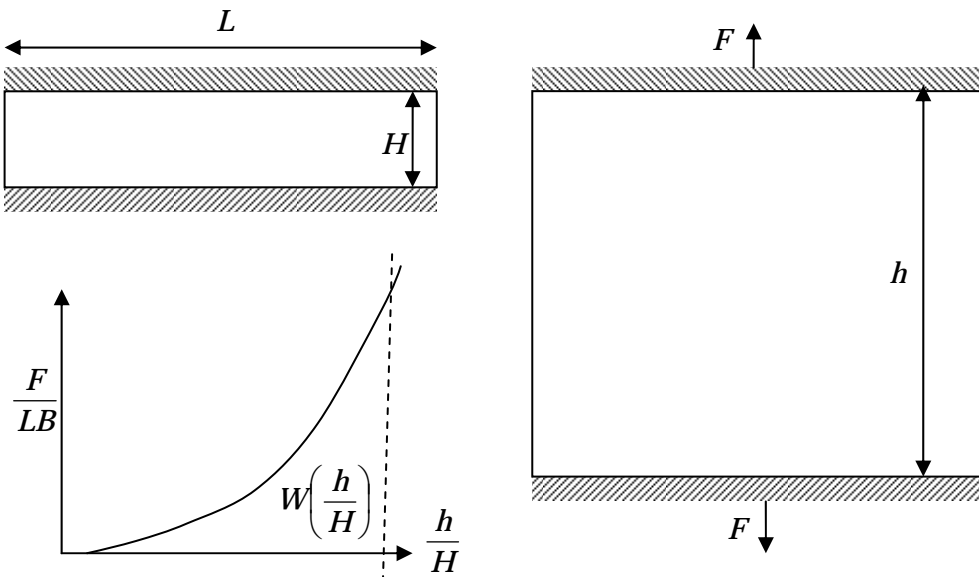
$$J = 2P\theta.$$

Andersson and Stigh (2004) used this result, to determine J as a function of δ_{tail} . Tamuzs, Tarasovs and Vilks (2003) compared several approximate formulas of J .

Crack bridging in soft materials. The crack-bridging model is applicable to soft materials. In particular, many soft tissues consist of fibers embedded in soft matrices. A specimen suitable to test soft materials is illustrated in the figure. A thin sheet is of dimension $H \times L \times B$ in the undeformed state. The sheet is fixed to two rigid grips, which are then pulled by a force F relative to each other to distance h . The specimen is called the pure-shear specimen.

The elastic energy density W is determined experimentally by the area of the stress-stretch curve. Write the energy density W as a function of the stretch h/H , namely,

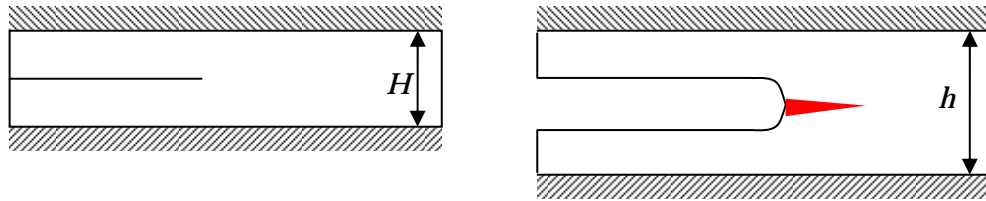
$$W = W\left(\frac{h}{H}\right).$$



Now cut the sheet with a crack before pulling the sheet. When the sheet with the pre-cut is pulled, the J integral over the external boundary is

$$J = HW\left(\frac{h}{H}\right).$$

It might be useful to observe the bridging zone and study it using the approaches described above.



The main theme of the crack-bridging model. A combination of micromechanical modeling and mechanical testing determines the traction-separation curve. Put the traction-separation curve into the continuum mechanics to predict macroscopic behavior/properties: toughness, strength, notch-sensitivity, etc. The model has related the macroscopic behavior to microscopic processes. It goes beyond the Griffith approach.

References

- T. Andersson and Stigh, The stress-elongation relation for an adhesive layer loaded in peel using equilibrium of energetic forces. *International Journal of Solids and Structures* 41, 413-434 (2004).
- B.A. Bilby, A.H. Cottrell, and K.H. Swinden, The spread of plastic yield from a notch. *Proceedings of the Royal Society of London A272*, 304-314 (1963).
- D.S. Dugdale, Yielding of steel sheets containing slits. *Journal of the Mechanics and Physics of Solids* 8, 100-104 (1960).
- I. Mohammed and K.M. Liechti, Cohesive zone modeling of crack nucleation at bimaterial corners. *Journal of the mechanics and physics of Solids* 48, 735-764 (2000).
- A.J. Paris and P.C. Paris, Instantaneous evaluation of J and C^* . *International Journal of Fracture* 38, R19-R21 (1988).
- S.M. Spearing and A.G. Evans, The role of fiber bridging in the delamination resistance of fiber-reinforced composites. *Acta Metall. Mater.* 40, 2191 (1992).
- B.F. Sorensen, Cohesive law and notch sensitivity of adhesive joints. *Acta Materialia*, 50, 1053-1061 (2002).
- B.F. Sorensen and T.K. Jacobsen. Large-scale bridging in composites: R-curves and bridging laws. *Composites Part A* 29, 1443-1451 (1998).
- Z. Suo, G. Bao and B. Fan, Delamination R-curve phenomena due to damage. *J. Mech. Phys. Solids.* 40, 1-16 (1992).
<http://www.seas.harvard.edu/suo/papers/015.pdf>
- Z. Suo, S. Ho and X. Gong, Notch ductile-to-brittle transition due to localized inelastic band, *ASME J. Engng. Mater. Tech.* 115, 319-326 (1993).
<http://www.seas.harvard.edu/suo/papers/031.pdf>
- M.D. Thouless, J.L. Adams, M.S. Kfkalidis, S.M. Ward, R.A. Dickie, G.L. Westerbeek, Determining the toughness of plastically deforming joints. *Journal of Materials Science* 33, 189-197 (1998).
- V. Tamuzs, S. Tarasovs, U. Viks, Progressive delamination and fiber bridging modeling in double cantilever beam composite specimens. *Engineering Fracture Mechanics* 68, 513-525 (2001).